Noise and Surface Pressure Response of an Airfoil to Incident Turbulence

Robert W. Paterson* and Roy K. Amiet†
United Technologies Research Center, East Hartford, Conn.

A theoretical and experimental investigation of the nosie and unsteady surface pressure characteristics of an isolated airfoil in a uniform mean velocity, homogeneous, nearly isotropic turbulence field was conducted. Experiments were performed with a 23-cm chord, two-dimensional, NACA 0012 airfoil in the UTRC Acoustic Research Tunnel over a Mach number range of 0.1 to 0.5. Far-field noise spectra and directivity as well as surface pressure spectra and cross-spectra were obtained. Incident turbulence statistics were documented. Theory applied to predict far-field noise and surface pressure characteristics from measured inflow turbulence statistics showed good agreement with measurement over the dominant frequency range for all Mach numbers investigated. The theoretical formulation represents a first-principles solution providing absolute level prediction without recourse to empirical or adjustable constants. It takes into account compressibility as well as source noncompactness effects. Correlation measurements demonstrated that all chordwise portions of the airfoil radiated directly to the far-field, but that the leading edge was the dominant noise producing region.

Nomenclature

b = airfoil semichord
c = airfoil chord
c_0 = speed of sound
d = airfoil semispan
f = frequency, Hz
g = pressure jump across airfoil normalized by $2\pi\rho_0 U w_0$
k_x, k_y, k_z = axial (chordwise), lateral (spanwise), and vertical (normal to airfoil) components of turbulence wavenumber vector
$\hat{k}$ = wavenumber normalized by k_e, k/k_e
k_e = wavenumber range of energy-containing eddies, $3/4\,\Lambda_f$
k_x^* = k_x/β^2
$\bar{k}_x^*$ = $k^*_x b$
$k_{x,y}$ = $k_{x,y} b$
K_x = ω/U
$\hat{K}_x$ = K_x/k_e
K_y = $\omega y/c_0\sigma$
$\mathfrak{L}$ = effective lift
M = Mach number
p_s = airfoil surface pressure
p = sound pressure
ΔP = pressure jump across airfoil
r = observer position
$R_{ww}(k_x, y)$ = spanwise cross-spectrum of velocity component w
$R_{ww}(k_x, 0)$ = one wavenumber spectrum (PSD) of velocity component w, $= \Phi_{ww}(k_x)$
$\tilde{R}_{ww}(k_x, y)$ = spanwise cross-spectrum of w normalized by $R_{ww}(k_x, 0)$
s = airfoil span
S = Sears function
S_{pp} = far-field sound power spectral density (two-sided)
$S_{qq}(x_1, x_2, \eta, \omega)$ = cross-PSD of airfoil surface pressure (two-sided)
u = axial turbulent velocity component
U = mean velocity in axial direction
w = vertical (normal to airfoil) turbulent velocity component
w_g = gust velocity normal to airfoil
w_0 = magnitude of gust velocity
x = axial Cartesian coordinate
$\bar{x}$ = x/b
y = lateral (spanwise) Cartesian coordinate
y^* = $yk_e(1+\hat{k}_x^2)^{1/2}$
$\hat{y}^*$ = $(4/3)y^*$
z = vertical (normal to airfoil) Cartesian coordinate
β^2 = $1-M^2$
η = spanwise separation distance
θ = directivity angle in x, z plane measured relative to downstream axis, $\theta = 180 - \phi$, deg
λ = acoustic wavelength
Λ_f = longitudinal space integral scale of turbulence
μ = $MK_x b/\beta^2$
ρ_0 = freestream density
σ^2 = $x^2 + \beta^2(y^2 + z^2)$
τ = time delay, μsec
ϕ_M = directivity angle in x, z plane measured relative to upstream axis, $\phi = 180 - \theta$, deg
$\Phi_{ww}(k_x, k_y)$ = two wavenumber spectrum of w
$\Phi_{ww}(k_x)$ = PSD of w
ω = circular frequency, rad/sec

Presented as Paper 76-571 at the 3rd AIAA Aero-Acoustics Conference, Palo Alto, Calif., July 20-23, 1976; submitted Aug. 20, 1976; revision received Jan. 17, 1977.
Index categories: Noise; Aeroacoustics.

*Supervisor, Aeroacoustics and Experimental Gas Dynamics Group. Member AIAA.
†Senior Research Engineer, Aeroacoustics and Experimental Gas Dynamics Group. Member AIAA.

Introduction

ACOUSTIC radiation by an airfoil due to incident turbulence is an important phenomenon, since it is both an effective noise generating mechanism and its occurence is widespread. The present study was undertaken to treat the stationary isolated airfoil problem in a rigorous theoretical manner and with an experimental configuration capable of direct assessment of theory. Although the theoretical foundation for studying this problem extends to the early unsteady airfoil theory development of von Kármán and Sears[1] and the acoustic formulation of Curle,[2] Sharland[3] in 1964 was the first to assess experimentally, and to attempt to predict, incident turbulence noise. Subsequent investigations were conducted by Potter,[4] Clark[5], Dean,[6] Goldstein,[7] and

Olsen.[7,8] The previous studies were limited in that the mean velocity and incident turbulence properties varied in the spanwise direction requiring a degree of arbitrariness in assigning a single spanwise average value for the purpose of noise prediction. In addition, the incident turbulence properties were either not measured or their documentation was incomplete. Fink's[9] recent study removed all of these experimental limitations with the exception that the spanwise cross-spectrum of the incident turbulence was not measured. In addition to these studies, Hersh and Meecham[10] measured an approximate dipole radiation pattern. Clark and Ribner[11] and Siddon[12] conducted correlation studies directed toward increased understanding of the funadmental noise generation process. From a theoretical standpoint, Liepmann,[13] Diederich,[14] and Ribner[15] studied the problem of lift response in unsteady flow. Because these early papers were concerned only with lift, they are limited in the extent to which they can be used to calculate noise generation. More recent treatments of the lift response problem (Jackson et al.[16] and Filotas[17]) and of far-field noise generation (Dean[6] and Mugridge[18]) assume incompressible flow. The approach used by Fink[9] does not have the low-frequency limitation, but is somewhat empirical compared to the approach used here. Kaji[19] treated the problem of acoustic radiation produced by an airfoil in response to a discrete gust, including non-compactness effects. Goldstein[20] derived results that are similar in many respects to those used here. However, by assuming compactness in the chordwise direction, that approach is limited to acoustic wavelengths that are significantly greater than a chord.

In the present study, the experimental and theoretical limitations discussed previously were not present. The simplest geometry of an isolated airfoil in a uniform, spanwise homogeneous, nearly isotropic turbulent field was employed. A large airfoil model (23-cm chord) permitted investigation of the important regime in which the simplifying assumption of acoustical compactness did not apply. All of the turbulence statistical parameters affecting radiated noise were measured. A more detailed report of this investigation is given elsewhere.[21,22]

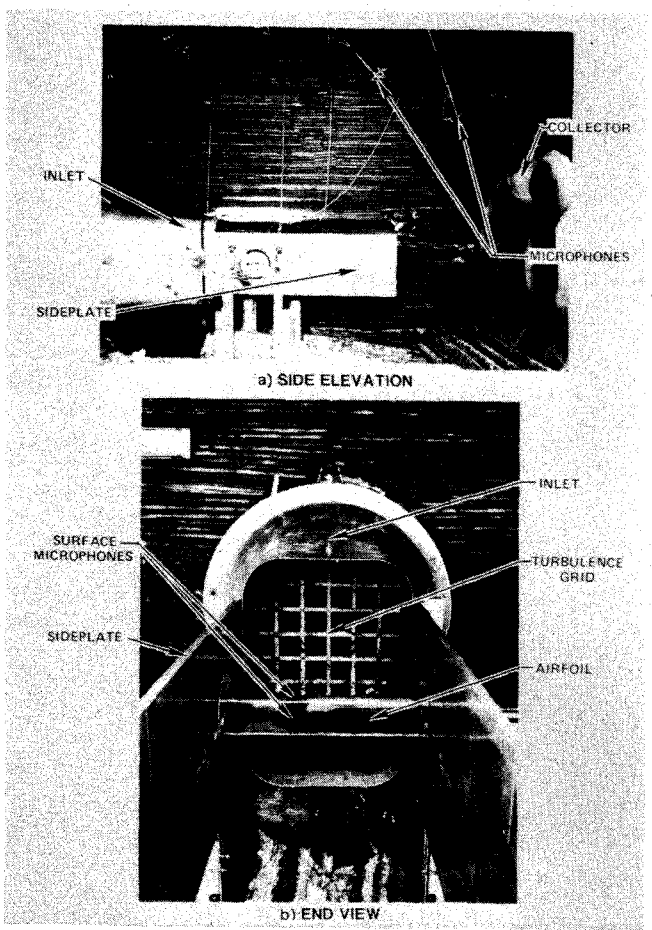

Fig. 1 Test section arrangement.

Description of the Experiment

This study was conducted in the UTRC Acoustic Research Tunnel which is described in detail elsewhere.[23] Propagation of airfoil noise through the open-jet shear layer causes refraction of sound wavefronts, which must be accounted for in data interpretation. Figure 1 displays the anechoic chamber test section arrangement employed in this study. The test airfoil was mounted horizontally between two vertical sideplates. The airfoil support permitted angle-of-attack variations. The sideplates provided two-dimensional flow conditions, and eliminated the need to extend the airfoil through the open-jet shear layer that would have existed in their absence. Far-field microphones were located on a 2.25-m radius arc, relative to the airfoil centerline, in a vertical plane on the tunnel centerline. A total of six far-field microphones were employed with angles relative to the upstream direction of 70, 90, 105, 120, 130, and 140 deg. The turbulence grid seen in this view was employed to generate turbulence incident on the test airfoil. The grid was located 1.22-m upstream of the inlet nozzle lip in a 1.07-m-diam section of the inlet contraction. The test airfoil shown in Fig. 1 was a 0.23-m chord, 0.53-m span, NACA 0012 airfoil. The model was instrumented with an array of four fixed and one movable flush-mounted condenser microphones on the airfoil upper surface. Four fixed microphones were located at one-third span and 15, 38, 50, and 70% chord, respectively. A microphone at 30% chord was housed in a slider capable of traverse over the complete span of the airfoil. This array permitted measurement of the local fluctuating surface pressure in both the span and chord directions. In this report, amplitudes of noise and surface pressure spectra are presented in terms of "spectrum level" (PSD), which is defined as the sound pressure level in decibels referred to 0.0002 μbar, based on a 1-Hz bandwidth analysis.

Definition of the Incident Turbulence Field

Acoustic radiation by an airfoil at an angle of attack of zero in the presence of inflow turbulence is associated with unsteady lift caused by the transverse turbulence component that is normal to both span and chord (in this experiment, the vertical component). At angle of attack, the axial component

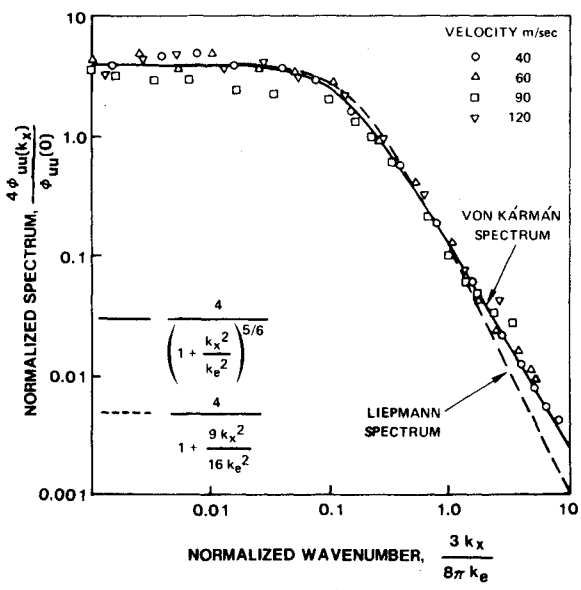

Fig. 2 One-dimensional spectrum of axial turbulence component.

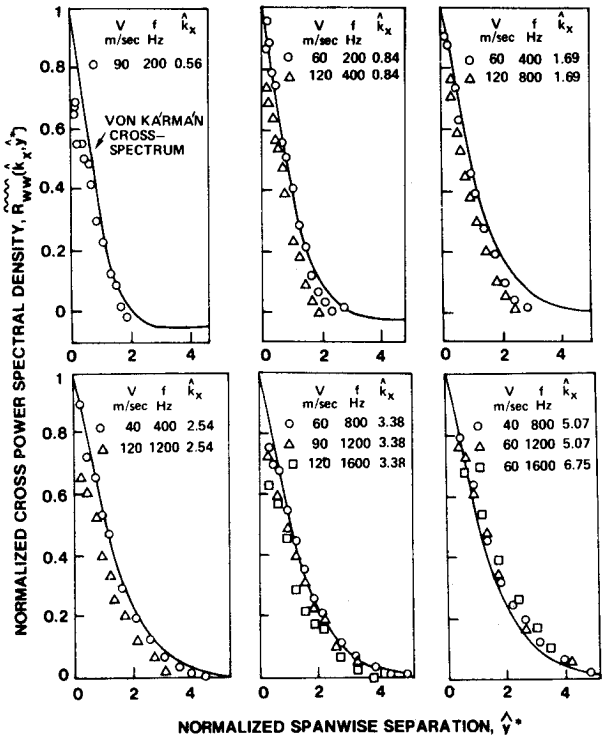

Fig. 3 Spanwise cross-spectrum of vertical turbulence component.

also affects lift. For the zero-angle-of-attack case, noise generation is dependent upon the distribution of intensity and axial length scale across the airfoil span, as well as the extent to which the vertical velocity component is correlated in the spanwise direction. Measurements, therefore, were required to establish the extent of spanwise uniformity (lateral homogeniety), spectra, axial length scale, and the cross-PSD of the vertical velocity component in the spanwise direction. Although prediction of overall sound pressure level would require only the overall spanwise cross-correlation of the vertical component, prediction of spectra requires knowledge of the spanwise cross-correlation as a function of frequency (i.e., spanwise cross-PSD).

As shown in detail in Ref. 21, the axial and vertical turbulence components were found to be homogeneous in the spanwise direction with the intensities of the two components nearly equal. The span average values of the vertical component intensities at tunnel speeds of 40, 60, 90, and 120 m/sec were 4.5, 3.9, 4.8, and 4.1%, respectively. Based on autocorrelations shown in Ref. 21, the longitudinal space integral scale Λ_f was found to be approximately 3 cm and relatively independent of tunnel speed. As shown in Fig. 2, the axial component spectra are in good agreement with the results that can be derived from the von Kármán interpolation formula for isotropic turbulence.[24] The results of additional turbulence measurements are given in Ref. 21. Shown in Fig. 3 are measurements of the spanwise cross-spectrum of the vertical turbulence velocity component for various test velocities and frequencies and as solid lines, the expression for the normalized spanwise cross-spectrum that can be derived from the von Kármán interpolation formula for isotropic turbulence:

$$\tilde{R}_{ww}(k_x,y) = [2^{1/6}/\Gamma(5/6)](y^*)^{5/6}[K_{5/6}(y^*) - [3y^*/(3+8\hat{k}_x^2)]K_{1/6}(y^*)] \quad (1)$$

In this expression, derived in Ref. 21, the K's denote modified Bessel functions of the second kind and fractional order, $\hat{k}_x$ is the ratio of axial wavenumber k_x to the wavenumber range of energy-containing eddies k_e and y^* is normalized spanwise separation distance. The data are well represented by the von Kármán expression, provided that the normalized separation is replaced by $\hat{y}^* = (4/3)y^*$. Based on these results it was concluded that the von Kármán expression employing $\hat{y}^*$ as the nondimensional separation constituted the appropriate spanwise cross-spectrum for use in the analytical prediction of surface pressures and far-field noise.

Far-Field Analyses and Results

Far-Field Noise Theory

The present approach is based on Ref. 25. The turbulence is assumed to be frozen and represented in terms of its spectral wavenumber components, k_x and k_y. The airfoil is assumed to be a flat plate of zero thickness, and linearized theory is assumed so that the wavenumber associated with the z coordinate normal to the airfoil (at zero angle of attack) does not enter. End effects are ignored in calculating the airfoil response (i.e., the airfoil surface pressure is calculated as if the airfoil were infinite). Effects of compressibility in the airfoil response function and noncompactness effects in calculation of the far-field sound are included. The assumption of large span allows simplification of the expression for far-field sound. The result for the overall lift under this approximation agrees with an expression given previously by other authors, being designated in those papers as "strip theory."[13,16] However, it was not clearly pointed out in these references that the result is mathematically rigorous in the large span limit and does not require the "strip theory" approximation. A similar approximation also was made by Goldstein.[7]

An airfoil of chord $2b$ and span $2d$ is placed in a turbulent fluid with a mean flow U in the axial (chordwise) direction. The y coordinate extends in the lateral (spanwise) direction, the z axis is vertical (normal to the airfoil), the origin of the coordinate system is at the center of the airfoil, and the observer is in the far-field. With this notation, the following expression for the far-field sound power spectral density applies[25]:

$$S_{pp}(r,\omega) = \left(\frac{\omega z \rho_0 b}{c_0 \sigma^2}\right)\pi U d \int_{-\infty}^{\infty} \left|\mathfrak{L}(r,K_x,k_y)\right|^2 \Phi_{ww}(K_x,k_y) \cdot \left[\frac{\sin^2[(k_y+K_y)d]}{\pi d(k_y+K_y)^2}\right] dk_y \quad (2)$$

where $\Phi_{ww}(k_x,k_y)$ is the two wavenumber spectrum, and the effective lift $\mathfrak{L}$ is given by

$$\mathfrak{L}(r,K_x,k_y) = \int_{-l}^{l} g(\xi,K_x,k_y)\exp - i\mu\xi(M - x/\sigma)\,d\xi \quad (3)$$

The normalized pressure jump across the airfoil g is defined as

$$\Delta P(x,y,t;K_x,k_y) = 2\pi\rho_0 U w_0 g(x,k_x,k_y) e^{i(k_x Ut - k_y y)} \quad (4a)$$

where ΔP is the pressure jump produced by a normal gust velocity

$$w_g = w_0 e^{i[k_x(Ut-x) - k_y y]} \quad (4b)$$

Also, the following quantities are defined:

$$K_x = \omega/U \qquad K_y = \omega y/c_0\sigma$$

$$\sigma^2 = x^2 + \beta^2(y^2+z^2) \qquad \mu = MK_x b/\beta^2 \qquad \beta^2 = 1 - M^2 \quad (4c)$$

In these expressions, k_x and k_y are the axial (chordwise) and lateral (spanwise) wavenumbers of the turbulence, respectively. Additional quantities are defined in the list of symbols. It should be noted that Eqs. (4a-4c) are the complex conjugates of the corresponding equations given in Ref. 25. This

results in a positive value $K_x = \omega/U$ rather than the negative value $K_x = -\omega/U$ of Ref. 25, when the time Fourier transform is defined as

$$F(\omega) = \frac{1}{2\pi}\int_{-\infty}^{\infty} f(t)e^{-i\omega t}\,dt \tag{4d}$$

The function $(\sin^2\xi d)/(\xi^2\pi d)$ in Eq. (2) behaves like a delta function of ξ for large d. As was shown in Ref. 25, when the acoustic wavelength λ is much smaller than the airfoil semispan d, Eq. (2) can be simplified to

$$S_{pp}(r,\omega) = \left(\frac{\omega z \rho_0 b}{c_0\sigma^2}\right)^2 \pi U d\,|\mathfrak{L}(r,K_x,K_y)|^2 \Phi_{ww}(K_x,K_y) \tag{5}$$

Under this limitation (which can be written $MK_x d \gg 1$), the airfoil loading becomes concentrated within the order of a wavelength from the airfoil leading edge, and finite span effects are limited to a distance on the order of a wavelength from the ends. Thus, under the limit $\lambda \ll d$, it is not necessary to assume large airfoil aspect ratio for Eq. (5) to hold. When the aspect ratio $\mathcal{R}$ is large, the restriction $MK_x d \gg 1$ can be relaxed to $K_x d \gg 1$. Under this restriction, end effects are limited to within a chordlength from the ends and again can be neglected. Equation (5) thus is exact for both the limits

$$MK_x d \to \infty \qquad \text{and} \quad K_x d \to \infty \text{ with } \mathcal{R} \to \infty \tag{6}$$

The airfoil response functions used to calculate $\mathfrak{L}$ will be approximations, one for the low-frequency regime and one for the high-frequency regime. Together they give good approximations to the airfoil response for all frequency, as discussed elsewhere.[26] For the low-frequency regime, $\mu < 0.4$, the solution of Amiet[27] is used. This small μ solution is correct to 0 (μ) and neglects terms 0 (μ^2) and higher. It is similar to the solution of Osborne,[28] which had neglected a term of 0 (μ). Further discussion of the solution is given in Refs. 26, 29, and 30. The solution for the pressure distribution produced by a gust given by Eq. (4b), with $k_y = 0$ on an airfoil situated between $-1 \le \bar{x} \le 1$, is shown in Ref. 27 to be

$$g(x,k_x,0) = \frac{1}{\pi\beta}\sqrt{\frac{1-\bar{x}}{1+\bar{x}}}\,S(\bar{k}_x^*)\,e^{i\bar{k}_x^*[M^2\bar{x}+f(M)]} \qquad \mu < 0.4 \tag{7a}$$

where

$$f(M) = (1-\beta)\ln M + \beta\ln(1+\beta) - \ln 2 \tag{7b}$$

and S is the classical Sears function.[1] The overbar indicates a variable nondimensionalized by the semichord b. The result for nonzero k_y, needed when the observer is not in the $y=0$ plane, can be obtained by using the similarity rules of Graham.[31] Introducing Eq. (7) into Eq. (3) gives

$$\mathfrak{L}(r,k_x,0) = (1/\beta)\,S(\bar{k}_x^*)\,[J_0(\mu x/\sigma) - iJ_1(\mu x/\sigma)]\,e^{i\bar{k}_x^* f(M)} \qquad \mu < 0.4 \tag{8}$$

Since only the absolute value is needed, this can be simplified. Equation (8) already ignores terms of 0 (μ^2). To be consistent, the absolute value of $J_0 - iJ_1$ can be approximated by 1, giving

$$|\mathfrak{L}| = (1/\beta)\,|S(\bar{k}_x^*)| \tag{9}$$

A simple, but accurate, approximation to the Sears function, which was used in the calculation, is

$$S(\bar{k}_x) \simeq [1/(1+2.4\bar{k}_x) + 2\pi\bar{k}_x]^{-1/2} \tag{10}$$

Although this approximation loses the logarithmic behavior of the Sears function for small k_x, the accuracy is quite good.

For high frequency, the solution used is that of Adamczyk, which was derived by an iteration procedure similar to that of Refs. 32 and 33. It consists of a series of corrections made alternately to the leading and trailing edges. The first two terms given by Adamczyk[34] will be used here. An alternate derivation and further comparison with numerical results is given in Refs. 26 and 35. The first term alone can be used for $\mu > 0.75$. Here the first two corrections will be used, which extends the range to $\mu > 0.4$; this is the changeover between the high- and low-frequency two-dimensional solutions used in the present calculations. The first two terms of the Adamczyk solution for the pressure jump g of an airfoil situated between $-1 \le \bar{x} \le 1$ are given in Refs. 26, 34, and 35 as (presented here are the $k_y = 0$ limits and the complex conjugate of the solutions given in Ref. 31; also, both Refs. 26 and 34 use different definitions of E):

$$g_1(x,k_x,0) = \frac{1}{\pi\sqrt{\pi(1+M)\bar{k}_x(1+\bar{x})}}$$
$$\exp\{-i[\mu(1-M)(1+\bar{x}) + \pi/4 - \bar{k}_x] \tag{11a}$$

$$g_2(x,k_x,0) \approx \frac{1}{\pi\sqrt{2\pi(1+M)\bar{k}_x}}\{(1+i)E^*[2\mu(1-\bar{x})] - 1\}$$
$$\exp\{-i[\mu(1-M)(1+\bar{x}) + \pi/4 - \bar{k}_x]\} \tag{11b}$$

$$g = g_1 + g_2 \qquad \mu > 0.4 \tag{11c}$$

where

$$E^*(x) = \frac{1}{\sqrt{2\pi}}\int_0^x e^{-i\xi}\frac{d\xi}{\sqrt{\xi}} \tag{12}$$

is a combination of Fresnel integrals.

Introducing Eqs. (11a and 11b) into Eq. (3) gives

$$\mathfrak{L}_1(r,k_x,0) = \frac{1}{\pi}\sqrt{\frac{2}{(1+M)\bar{k}_x\Theta_1}}\,E^*(2\Theta_1)\,e^{i\Theta 2} \tag{13a}$$

$$\mathfrak{L}_2(r,k_x,0) \approx \frac{1}{\pi\Theta_1\sqrt{2\pi(1+M)\bar{k}_x}}\,e^{i\Theta 2}\Big(i(1-e^{-i2\Theta 1})$$
$$+ (1-i)\{E^*(4\mu) - \sqrt{\frac{2}{1+x/\sigma}}\,e^{-i2\Theta 1}E^*[2\mu(1+\frac{x}{\sigma})]\}\Big) \tag{13b}$$

$$\mathfrak{L} = \mathfrak{L}_1 + \mathfrak{L}_2 \tag{13c}$$

where $\Theta_1 \equiv \mu(1 - x/\sigma)$ and $\Theta_2 \equiv \bar{k}_x^*(1 - Mx/\sigma) - \pi/4$. For use in Eq. (5), Eqs. (13a) and (13b) first are added, and then the absolute value is taken, whereupon the function Θ_2 drops out.

Equations (5, 9, 10, 12, and 13), in conjunction with the von Kármán two wavenumber spectrum of the vertical velocity component of the turbulence $\Phi_{ww}(k_x,k_y)$ (Ref. 21 or 25), are those used in the present study to predict far-field noise in the $y=0$ plane. In comparing with experimental data, the physically realizable one-sided PSD, defined for positive frequencies only $G_{pp} = 2S_{pp}$, is employed, and a factor of 2π is accounted for in expressing results in terms of unit frequency rather than unit circular frequency.

Shear Layer Refraction Effects

In order to compare with data, a correction must be applied to account for refraction by the tunnel shear layer. For this purpose, the open-jet wind tunnel refraction corrections of Amiet[36] were used. This necessitates both a directivity angle and an amplitude correction. Rather than correct the data, however, the data were left "as measured" and the corrections were applied to the theory in order to find predicted

sound levels in the presence of the shear layer. Plots of the corrections, which were applied to the theoretical results, are given in Refs. 21 and 22.

Airfoil Response Function Compressibility Effects

The importance of using airfoil response functions that include the effect of compressibility is discussed in Refs. 21 and 22. The results of a calculation that uses the airfoil response functions that include compressibility are compared with the same calculations using the incompressible airfoil response function (the classical Sears function) times the Prandtl-Glauert factor $1/\beta$. The results agree closely at low frequency as would be expected, but at high frequency the difference can be significant.

Directivity and Velocity Dependence

References 21 and 22 discuss the effect of frequency on the sound directivity pattern and demonstrate the importance of accouting for noncompactness effects at high frequency. It also is shown that, if the percent turbulence level and the axial wavenumber $K_x\ (=\omega/U)$ are kept fixed as U is varied, and M is small, the acoustic energy in a fixed percent frequency bandwidth behaves as U^6 at low frequency and U^5 at high frequency. These simple relationships do not hold at non-negligible Mach number.

Comparison of Theoretical and Experimental Spectral Results

Shown in Fig. 4 is a comparison between theory and experiment for the noise spectra directly above the airfoil at an airfoil angle of attack of zero. The directivity angle ϕ_M is the angle relative to the upstream direction, and therefore is 90 deg for this case $(\phi = 180 - \theta)$. The data represent measurement at 90 deg in the presence of the tunnel shear layer. The theoretical predictions shown by solid lines include the shear layer refraction correction discussed previously and therefore can be compared directly to measured data acquired in the presence of the tunnel shear layer. The experimental data points have been obtained by subtracting measured tunnel background noise from the measured spectra. Flagged symbols denote data points for which the difference between airfoil and background noise was between 4.3 and 2.2 dB, thus requiring corrections of 2 to 4 dB in measured airfoil levels. These data are subject to greater uncertainty than are unflagged points for which corrections of less than 2 dB were required. Data requiring corrections greater than 4 dB have not been plotted, since an uncertainty greater than one or two decibels in absolute level could exist.

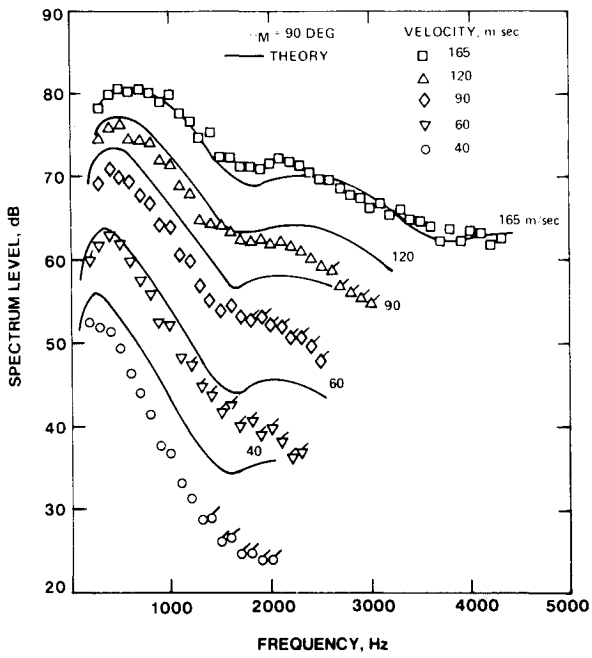

Fig. 4 Comparison of measured and theoretically predicted far-field noise spectra.

The agreement between theory and experiment is considered good, particularly for the low-frequency noise that dominates the spectra, and for the high Mach numbers most relevant to helicopter rotor, propeller, and turbomachinery noise. Significant deviations between theory and experiment generally are observed at high frequency with the disagreement greatest at low velocity. Such behavior would be expected because of finite airfoil thickness effects not accounted for by the theory. When the gust wavelength decreases to a length comparable to the airfoil thickness in the vicinity of the leading edge, significant errors would be anticipated. Since gust wavelength is given by the ratio of mean velocity to frequency, an order-of-magnitude criterion for breakdown of theory can be expressed as $U/ft_A \leq 1$, where f is sound frequency, U the velocity, and t_A the airfoil thickness. The observed disagreement is approximately 5 dB when the previous equality is satisfied. Although a rigorous explanation for this breakdown cannot be given, an eddy, small in comparison with a leading-edge thickness dimension, would not be expected to produce the airfoil lift fluctuation that would obtain if the airfoil had zero thickness, and consequently appeared to the eddy as a knife edge. An implication of this result is that noise reductions greater than those predicted by theory may be achieved by reducing the ratio of turbulence scale to thickness.

Comparison of Theoretical and Experimental Directivity Results

Shown in Fig. 5 is a comparison between theory and experiment for the far-field airfoil noise directivity as a function of frequency at an airfoil angle of attack of zero. The agreement is observed to be good, except for low values of U/ft_A, as in the case of the 90-deg spectral comparison. Of interest is the theoretical prediction of a progression from a smooth directivity pattern nearly symmetrical with 90 deg at low frequency to an aft-quadrant-dominated wavy pattern at high frequency. This is partially confirmed by the data. Both of the previous effects are attributed to source noncompactness at high frequency, as discussed in Refs. 21 and 22.

Surface Pressure Analyses and Results

Surface Pressure Theory

The airfoil surface pressure for any frequency can be found by summing the airfoil response to all of the spectral gust components contributing to that frequency. As given by Eq. (11) of Ref. 25, the cross-PSD of the surface pressure S_{qq} is

$$S_{qq}(x_1,x_2,\eta,\omega) = 2U(\pi\rho_0)^2 \int_0^\infty g^*(x_1,K_x,k_y)\, g(x_2,K_x,k_y)\cdot\Phi_{ww}(K_x,k_y)\cos(k_y\eta)\,dk_y \qquad (14)$$

For the calculation of far-field noise it was possible to simplify the k_y integral in Eq. (2). This is because an integral over the span was taken, resulting in a cancelling effect for all k_y spectral components except the one giving the entire noise contribution at that particular observer position. In calculating unsteady surface pressure, the absence of an integral over span means that the k_y integral cannot be simplified. Thus, the integration in Eq. (14) was carried out numerically to obtain the predictions of surface pressure cross-PSD. For large spanwise separation η, the integrand in Eq. (14) oscillates rapidly. For this reason Filon's method was used.[37] The approximate results used for the parallel compressible gust are the same as those used in the calculation of far-field noise. As for the parallel gust case, the calculation for the skewed incompressible gust was divided into two regimes: small k_y and large k_y. The solution for small k_y is

that of Amiet,[38] which gives, for the normalized pressure jump on an airfoil between $-1 \le \bar{x} \le 1$,

$$g(x,k_x,k_y) = \frac{1}{\pi} S(\bar{k}_x)\sqrt{\frac{1-\bar{x}}{1+\bar{x}}}\exp[i\bar{k}_x f'(k_y/k_x)]\,\bar{k}_y < 0.3 \quad (15a)$$

where

$$f'(\xi) = (\sqrt{1+\xi^2}-1)(i\pi/2 - \ln\xi) + \sqrt{1+\xi^2}\ln(1+\sqrt{1+\xi^2}) - \ln 2 \quad (15b)$$

The solution for large k_y, as for the parallel gust case, was obtained using the Schwartzschild-Landahl iteration technique. This solution is, in fact, mathematically related to the result for the parallel compressible gust case through the similarity rules of Graham,[31] just as the previous small k_y solution is related to the small μ solution. The first two terms given by Adamczyk[34] were shown in Ref. 35 to be quite accurate for $k_y > 0.25$ when compared with the numerical results of Graham.[39] For the present calculations, the two-term solution was used over the range $k_y > 0.3$. For an airfoil situated between $-1 \le \bar{x} \le 1$, the solution is

$$g_1(x,k_x,k_y) = \{1/[\pi\sqrt{\pi(\bar{k}_y + i\bar{k}_x)(1+\bar{x})}]\}e^{-\bar{x}\bar{k}_y + i\bar{k}_x} \quad (16a)$$

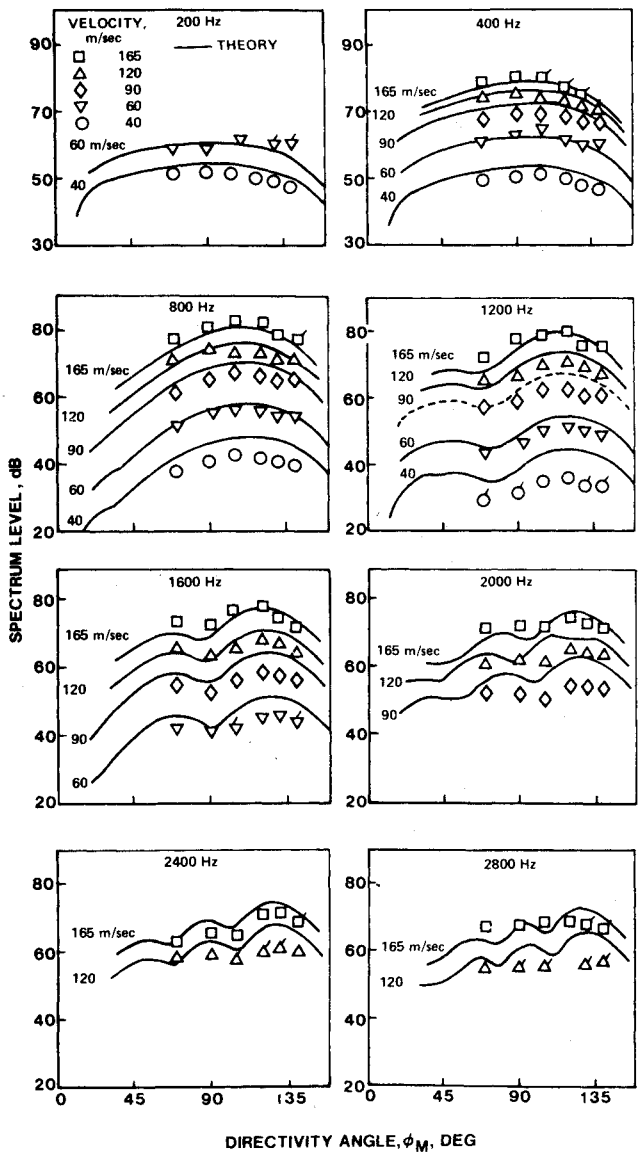

Fig. 5 Comparison of measured and theoretically predicted far-field noise directivity.

$$g_2(x,k_x,k_y) = \{1/[\pi\sqrt{2\pi(\bar{k}_y + i\bar{k}_x)}]\}\{\mathrm{erf}[\sqrt{2\bar{k}_y(1-\bar{x})}] - 1\}e^{-\bar{x}\bar{k}_y + i\bar{k}_x} \quad (16b)$$

Although Adamczyk gives the response function for a skewed compressible gust directly, this was broken down into the parallel compressible gust result [Eq. (11)] and the skewed incompressible gust result [Eq. (16)], since these were the limiting cases that were checked against numerical results. Graham's[31] similarity rules then were used to relate the general skewed compressible gust case to one of these two simpler results. This gives a more precise understanding of the accuracy to be expected of the general solution. The approximate solutions used herein are compared with exact numerical results in Ref. 21, showing that the approximate solutions are accurate to within a few percent of the exact solutions. Introducing these airfoil solutions into Eq. (14), along with the von Kármán two wavenumber spectrum (Refs. 21 or 25), allows calculation of the cross-spectrum of the surface pressure.

Comparison of Theoretical and Experimental Spectral Results

Shown in Fig. 6 is a comparison between theory and experiment for the airfoil chordwise unsteady surface pressure distribution as a function of frequency at an airfoil angle-of-attack of zero. The theoretical predictions shown by solid lines indicate a strong increase in unsteady pressure near the leading edge, suggesting that this is the dominant noise producing region of the airfoil. This strong increase near the leading edge is confirmed by the data. The agreement between theory and experiment, typically within several dB, is good considering the absolute level nature of the prediction method. The significant disagreement at 30% chord, noted at several frequencies, is believed to be related to transitional boundary-layer phenomena, as discussed in Ref. 21. References 21 and 22 also show a comparison between theory and experiment for the airfoil surface pressure spanwise cross-spectrum between the 15 and 30% chord microphones as a function of frequency at an airfoil angle-of-attack of zero. The agreement between theory and experiment was reasonable, considering the absolute level nature of the predictions.

Correlation Studies

Figure 7 shows typical surface-far-field auto and cross-correlation functions for the far-field microphone located directly above the airfoil (90 deg position) and the five surface microphones arrayed in the chordwise direction at a velocity of 120 m/sec. In the cross-correlations shown in this figure, positive delay time corresponds to delay of the surface microphone signal with respect to the far-field microphone signal. Cross-correlations between the far-field position and all chordwise microphones display a zero crossing between 6440 and 6520 μsec, which is close to the calculated acoustic propagation time from the center of the airfoil to the far-field microphone of 6475 μsec. This demonstrated that each of the measured chordwise positions was radiating noise directly to the far-field. Similar experimental results and this conclusion were reported by Fink in incident turbulence studies conducted with a flat plate.[9] Siddon also obtained identical cross-correlation zero crossings for various surface measurement locations.[12]

In addition to these time delay arguments, surface-to-far-field correlations can be employed to obtain quantitative information on the chordwise distribution of noise source strengths as shown by Siddon.[12] As discussed in Refs. 21 and 22, application of this method demonstrated that the dominant source of noise was the airfoil leading-edge region.

Angle of Attack Effects

Increase of airfoil geometric angle-of-attack from 0 to 8 deg was found to cause a small increase in far-field noise 90-deg at some frequencies (1 or 2 dB), and a somewhat larger increase

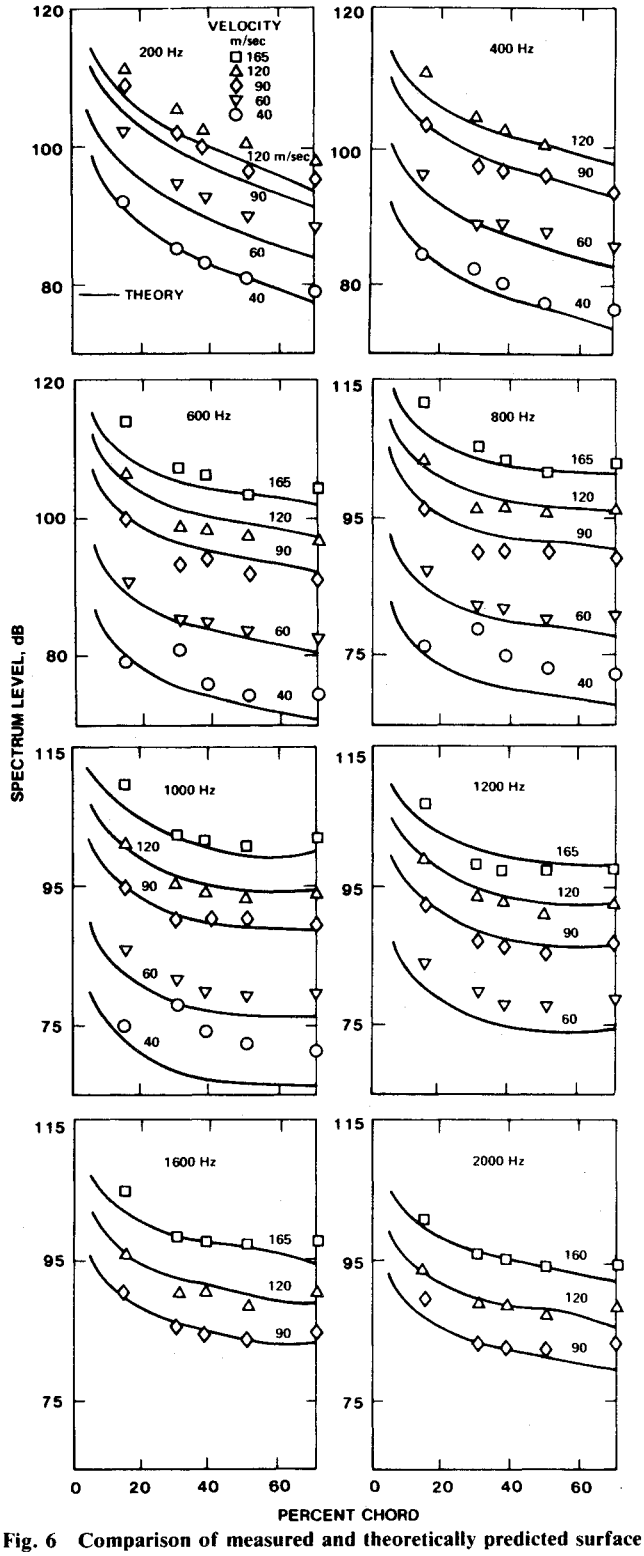

Fig. 6 Comparison of measured and theoretically predicted surface pressure distributions.

in surface pressure level. Dean[6] and Clark[5] also reported little or no dependence on angle-of-attack. Although a rigorous theoretical treatment of the angle-of-attack problem is not available presently, theoretical considerations described in Ref. 21 suggest that angle-of-attack effects on noise and surface pressures should be relatively small.

Approximate Expressions for Far-Field Noise

References 21 and 22 provide approximate expressions for incident turbulence far-field noise based on the full

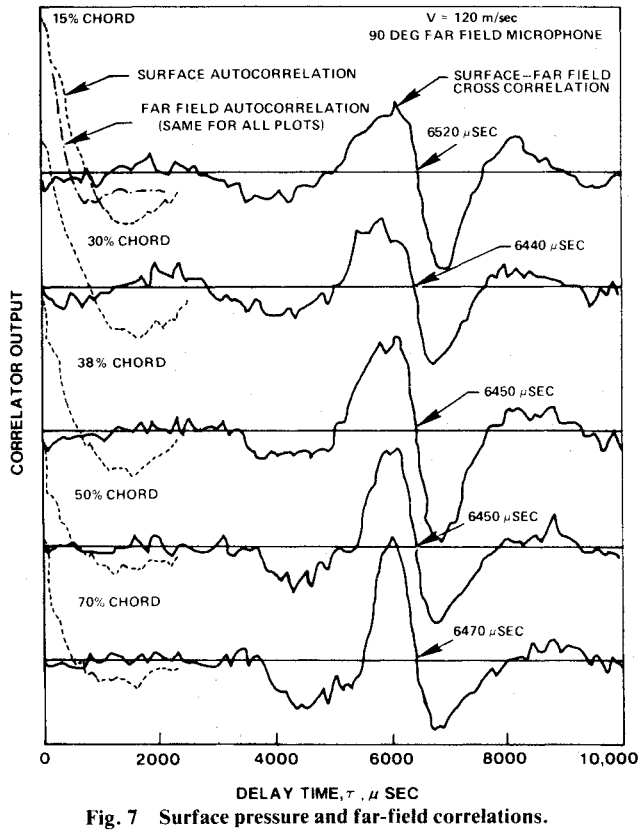

Fig. 7 Surface pressure and far-field correlations.

theoretical development given in the text. These expressions, although not exact, facilitate engineering calculations.

Conclusions

1) Incident turbulence is an important airfoil broadband noise mechanism. Its relative importance in full-scale applications would depend upon the intensity and scale of the incident turbulence flowfield.

2) A theory capable of absolute level prediction of airfoil far-field noise spectra, directivity characteristics, surface pressure spectra, and surface cross-spectra from incident turbulence properties, without use of empirical or adjustable constants, has been validated by experimental data.

3) The airfoil chordwise unsteady surface pressure distribution in incident turbulence is strongly peaked toward the leading edge. Although all chordwise positions radiate directly to the far-field, the leading-edge region is the dominant source of noise.

4) The effect of angle-of-attack on turbulence-induced far-field noise and airfoil surface pressures is small but measurable.

5) Inclusion of compressibility and source noncompactness effects in the theoretical formulation is necessary to obtain accurate amplitude and directivity predictions. Finite airfoil thickness effects are important at high frequency and low velocity.

6) An existing open-jet wind tunnel shear layer refraction correction procedure appears to account accurately for refraction effects on sound propagation.

Acknowledgment

The study reported herein was funded by NASA Langley Research Center under Contract No. NAS1-13823. The authors wish to acknowledge helpful discussions with R. N. Hosier and R. Pegg, NASA Langley, regarding the design and conduct of the experiment as well as correspondence with J.M.R. Graham, Imperial College, London, relative to definition of the incident turbulence field.

References

[1] von Kármán, T. and Sears, W. R., "Airfoil Theory for Non-Uniform Motion," *Journal of the Aeronautical Sciences*, Vol. 5, Aug. 1938, pp. 379-390.

[2] Curle, S. N., "The Influence of Solid Boundaries Upon Aerodynamic Sound," *Proceedings of the Royal Society*, Vol. A231, Sept. 1955, pp. 505-514.

[3] Sharland, I. J., "Sources of Noise in Axial Flow Fans," *Journal of Sound and Vibration*, Vol. 1, March 1964, pp. 302-322.

[4] Potter, R. C., "An Experiment to Examine the Effects of Porous Trailing Edges on the Sound Generated by Blades in an Airflow," NASA CR-66565, 1968.

[5] Clark, L. T., "Results of an Experimental Investigation Relating Sound Generation by a Single Airfoil in a Turbulent Flow," The Boeing Co., Rept. D6-23274, 1969.

[6] Dean, L. W., "Broadband Noise Generated by Airfoils in Turbulent Flow," AIAA Paper 71-587, June 1971.

[7] Goldstein, M. E., "Aeroacoustics," NASA SP-346, 1974, pp. 209-219.

[8] Olsen, W. A., "Noise Generated by Impingement of Turbulent Flow on Airfoils of Varied Chord, Cylinders and Other Flow Obstructions," AIAA Paper 76-504, July 1976.

[9] Fink, M. R., "Investigation of Scrubbing and Impingement Noise," NASA CR-134762, 1975.

[10] Hersh, A. S. and Meecham, W. C., "Sound Directivity Pattern Radiated from Small Airfoils," *Journal of the Acoustical Society of America*, Vol. 53, Feb. 1973, pp. 602-606.

[11] Clark, P.J.F. and Ribner, H. S., "Direct Correlation of Fluctuating Lift With Radiated Sound for an Airfoil in Turbulent Flow," *Journal of the Acoustical Society of America*, Vol. 46, Sept. 1969, pp. 802-805.

[12] Siddon, T. E., "Surface Dipole Strength by Cross-Correlation Method," *Journal of the Acoustical Society of America*, Vol. 53, Feb. 1973, pp. 619-633.

[13] Liepmann, H. W., "Extension of the Statistical Approach to Buffeting and Gust Response of Wings of Finite Span," *Journal of the Aeronautical Sciences*, Vol. 22, March 1955, pp. 197-200.

[14] Diederich, F. W., "The Dynamic Response of a Large Airplane to Continuous Random Atmospheric Disturbances," *Journal of the Aeronautical Sciences*, Vol. 23, Oct. 1956, pp. 917-930.

[15] Ribner, H. S., "Spectral Theory of Buffeting and Gust Response: Unification and Extension," *Journal of the Aeronautical Sciences*, Dec. 1956, pp. 1075-1077, 1118.

[16] Jackson, R., Graham, J.M.R., and Maull, D. J., "The Lift on a Wing in a Turbulent Flow," *Aeronautical Quarterly*, Aug. 1973, pp. 155-166.

[17] Filotas, L. T., "Theory of Airfoil Response in a Gusty Atmosphere. Part II-Response to Discrete Gusts or Continuous Turbulence," University of Toronto Institute Aerospace Studies, Rept. 141, 1969.

[18] Mugridge, B. D., "Sound Radiation from Airfoils in Turbulent Flow," *Journal of Sound and Vibration*, Vol. 13, Nov. 1970, pp. 362-363.

[19] Kaji, S., "Noncompact Source Effect on the Prediction of Tone Noise from a Fan Rotor," *Progress in Astronautics and Aeronautics*, Vol. 44, edited by I. R. Schwartz, MIT Press, 1976, pp. 55-82.

[20] Goldstein, M., *Aeroacoustics*, McGraw-Hill, New York, 1976, Chap. 3.

[21] Paterson, R. W. and Amiet, R. K., "Acoustic Radiation and Surface Pressure Characteristics of an Airfoil Due to Incident Turbulence," NASA CR-2733, 1976.

[22] Paterson, R. W. and Amiet, R. K., "Acoustic Radiation and Surface Pressure Characteristics of an Airfoil Due to Incident Turbulence," AIAA Paper 76-571, 1976.

[23] Paterson, R. W., Vogt, P. G., and Foley, W. M., "Design and Development of the United States Research Laboratories Acoustic Research Tunnel," *Journal of Aircraft*, Vol. 10, July 1973, pp. 427-433.

[24] Hinze, J. O., *Turbulence*, McGraw-Hill, New York, 1959.

[25] Amiet, R. K., "Acoustic Radiation from an Airfoil in a Turbulent Stream," *Journal of Sound and vibration*, Vol. 41, Aug. 1975, pp. 407-420.

[26] Amiet, R. K., "Effects of Compressibility in Unsteady Airfoil Lift Theories," in *Unsteady Aerodynamics*, edited by R. B. Kinney, University of Arizona/AFOSR Symposium, March 18-20, 1975, Tucson, Ariz., pp. 631-653.

[27] Amiet, R. K., "Compressibility Effects in Unsteady Thin-Airfoil Theory," *AIAA Journal*, Vol. 12, Feb. 1974, pp. 252-255.

[28] Osborne, C., "Unsteady Thin Airfoil Theory for Subsonic Flow," *AIAA Journal*, Vol. 11, Feb. 1973, pp. 205-209.

[29] Amiet, R. K., "Low Frequency Approximations in Unsteady Small-Perturbation Subsonic Flows," *Journal of Fluid Mechanics*, Vol. 75, June 1976, pp. 545-552.

[30] Kemp, N. H. and Homicz, G., "Approximate Unsteady Thin-Airfoil Theory for Subsonic Flow," *AIAA Journal*, Vol. 14, Aug. 1976, pp. 1083-1089.

[31] Graham, J.M.R., "Similarity Rules for Thin Aerofoils in Nonstationary Flows," *Journal of Fluid Mechanics*, Vol. 43, Oct. 1970, pp. 753-756.

[32] Schwartzschild, K., "Die Bengung and Polarisation des Lichts Durch Einen Spalt-I," *Math. Ann.*, Vol. 55, 1901, pp. 177-247.

[33] Landahl, M., *Unsteady Transonic Flow*, Pergamon Press, New York, 1961.

[34] Adamczyk, J. J., "The Passage of an Infinite Swept Airfoil Through an Oblique Gust," *Journal of Aircraft*, Vol. 11, May 1974, pp. 281-287.

[35] Amiet, R. K., "High Frequency Thin-Airfoil Theory for Subsonic Flow," *AIAA Journal*, Vol. 14, Aug. 1976, pp. 1076-1082.

[36] Amiet, R. K., "Correction of Open Jet Wind Tunnel Measurements for Shear Layer Refraction," *Progress in Astronautics and Aeronautics*, Vol. 46, edited by I. R. Schwartz, MIT Press, 1976, pp. 259-280.

[37] Hamming, R. W., *Numerical Methods for Scientists and Engineers*, McGraw-Hill, New York, 1962.

[38] Amiet, R. K., "Airfoil Response to an Incompressible Skewed Gust of Small Spanwise Wavenumber," *AIAA Journal*, Vol. 14, April 1976, pp. 541-542.

[39] Graham, J.M.R., "Lifting Surface Theory for the Problem of an Arbitrarily Yawed Sinusoidal Gust Incident on a Thin Airfoil in Incompressible Flow," *Aeronautical Quarterly*, Vol. 21, May 1970, pp. 182-198.